

Upper limits on *K*-band polarization in three high-redshift radio galaxies: 53W091, 3C 441 and MRC 0156–252

G. Leyshon,^{1,3} J. S. Dunlop^{2,4} and Stephen A. Eales^{1,5}

¹Department of Physics and Astronomy, Cardiff University, P.O. Box 913, Cardiff CF2 3YB

²Institute for Astronomy, Department of Physics and Astronomy, The University of Edinburgh, Edinburgh EH9 3HJ

³G.Leyshon@astro.cf.ac.uk ⁴J.Dunlop@roe.ac.uk ⁵S.Eales@astro.cf.ac.uk

19 November 2018

ABSTRACT

We present the results of *K*-band imaging polarimetry of three radio galaxies, including the very red and apparently old $z = 1.55$ galaxy 53W091. We find weak evidence for polarization in components of 3C 441 and in the south-east companion of 53W091, but no evidence of significant polarization in 53W091 itself. We also find strong evidence that MRC 0156–252 is unpolarised. We present upper limits for the *K*-band polarization of all three sources. For 53W091, the lack of significant *K*-band polarization provides further confidence that its red $R - K$ colour can be attributed to a mature stellar population, consistent with the detailed analyses of its ultraviolet spectral-energy distribution which indicate a minimum age of 2–3.5 Gyr.

Key words: infrared: galaxies – polarization – galaxies: active – galaxies: individual: LBDS 53W091 – MRC 0156–252 – 3C 441

1 INTRODUCTION

The visible and infrared light emitted by radio galaxies is thought to be a combination of starlight and nebular emission from the host galaxy, and a scattered power-law component originating in the active nucleus hidden in the heart of the galaxy. Manzini & di Serego Alighieri (1996) have examined a small sample of radio galaxies at redshifts ranging from 0.11 to 2.63, and have demonstrated that their observed magnitudes (by multiwaveband photometry) are consistent with spectra synthesised from three such components.

The Unified Model of radio-loud quasars and radio galaxies (Robson 1996, and references therein) suggests that both species contain an active nucleus consisting of an accretion disc shrouded in a dusty torus, with jets emerging at either pole. Those sources with jets oriented perpendicular to our line of sight are seen as radio galaxies with extended radio lobes but with their optical nuclear light shrouded, while those viewed ‘down the jet’ are classed as brilliant quasars with strong emission lines. It is now thought that some apparent ‘radio galaxies’, such as 3C 22 (Rawlings et al. 1995; Dunlop & Peacock 1993), may be in the quasar orientation, but with opaque material obscuring much of the light from the active nucleus.

It has been known for a decade that visible light from high- z radio galaxies is often aligned with the radio axis (Chambers, Miley & van Breugel 1987; McCarthy et al. 1987) – the so-called ‘alignment effect’ – and that this light

is often polarized with its *E*-vector oriented perpendicular to the radio axis (di Serego Alighieri et al. 1989; Jannuzzi & Elston 1991; Tadhunter et al. 1992). Both of these effects can be explained if the visible light is dominated by the nuclear component: nuclear light escapes from the active nucleus in a narrow cone about the radio jet, and a fraction is scattered towards us by dust or electrons. The scattering region forms an extended optical structure approximately parallel to the radio jet, and the scattered light becomes polarised perpendicular to the optical structure in the scattering process. Recent Keck spectropolarimetry by Cimatti et al. (1996; 1997; 1998), Dey et al. (1996) and Tran et al. (1998) have confirmed the presence of continuum light and broad lines in the polarized spectra of radio galaxies at $1.0 \lesssim z \lesssim 2.5$, with the polarization orientation being approximately perpendicular to the optical structure.

Manzini & di Serego Alighieri (1996) model radio galaxy spectra at rest frame wavelengths from 0.2 μm to 1.0 μm . The contribution of the starlight becomes greater at longer wavelengths, while the scattered nuclear component decreases. For five out of their six galaxies, the stellar component of the light has become dominant by a rest-frame wavelength of 0.5 μm ; in 3C 277.2 ($z = 0.766$) the starlight only exceeds the nuclear component at about 0.85 μm .

K-band observations of radio galaxies at $z \sim 1$ image light emitted at $\lambda \sim 1.1 \mu\text{m}$ in the rest frame. It is not obvious, *a priori*, that non-stellar features will be visible in this band; in practice, however, the alignment effect has

been detected in the infrared (Dunlop & Peacock 1993), albeit sometimes weakly (Rigler et al. 1992). It is now known that a substantial fraction of the K -band emission arises in the active nuclei of the most radio-loud galaxies, namely 3C sources and their southern hemisphere equivalents (Eales et al. 1997).

The first measurements of the K -band polarizations of high-redshift radio galaxies were carried out by Leyshon and Eales (1998) (hereafter L&E) in 1995. They found evidence for polarization in 3 out of 7 galaxies, and tentative evidence in two further cases. The galaxies formed a representative sub-sample of the 3C catalogue: polarization values ranged from 3 to 12 per cent, suggesting that up to a third of the K -band emission from such galaxies could originate in the active nucleus.

In their first study, L&E found that their two optically compact sources (3C 22 and 3C 41) gave the expected perpendicular alignment, but their extended sources (3C 114 and 3C 356) gave roughly parallel alignments, within rather large directional error bars. In this paper we continue our programme of K -band polarimetry with further observations of 3C 441, and polarimetry of MRC 0156–252 and the very red ($R - K = 5.8$) $z = 1.55$ milli-Jy radio galaxy LBDS 53W091.

2 TARGET OBJECTS

The study of K -band polarizations of distant, faint, radio galaxies is very much in its infancy. Our first paper (L&E) concentrated on 3C radio galaxies at $z \sim 1$. In this new study, we have extended our investigation to higher redshifts, choosing two targets with very different radio luminosities.

Galaxy LBDS 53W091 has a very low radio luminosity, which suggests the presence of a very weak active nucleus; but there is an unpublished claim (Chambers, private communication) of a ~ 40 per cent H -band polarization. Radio galaxy MRC 0156–252 has a high radio luminosity and infrared spectroscopy (see below) suggests that a large fraction of its K -band light may originate in an active nucleus. We also observed 3C 441, for which previous observations (L&E) had returned marginal results.

2.1 LBDS 53W091

The galaxy LBDS 53W091 (Figure 1) has aroused great excitement in the last two years. First investigated by Dunlop et al. (1996) as an extremely red radio-source identification, it was found to be a very red radio galaxy visible at high ($z = 1.552$) redshift. Its spectrum exhibits late-type absorption features, and no prominent emission features. The lack of emission features suggests that the active nucleus responsible for its ~ 25 mJy 1.4 GHz radio emission contributes very little light to the visible/ultraviolet, and consistent with this Spinrad et al. (1997) note that radio galaxies with weak active nuclei ($S_{1.4\text{GHz}} < 50$ mJy) generally are not expected to be dominated by optical nuclear emission, and do not display the alignment effect (their 4.86 GHz radio map of 53W091 reveals a double-lobed FR-II steep spectrum radio source, where the radio lobes are separated by approximately $4''3$ at position angle 131°).

Dunlop et al. (1996) argue that the galaxy is unlikely to be an obscured quasar and that its red colour $R - K = 5.8$ is due to its mature stellar population. This is based on a detailed investigation of its rest-frame ultraviolet spectral energy distribution. This appears essentially identical to that of an F5V star, indicating that stars of spectral type younger than approximately F2 have all evolved off the main-sequence (Dunlop et al. 1996).

The importance of 53W091 is therefore that, despite being initially discovered as a weak radio source, it is currently the best example of a red elliptical at $z > 1.5$ whose colours appear to be entirely due to an ‘old’ stellar population. Thus, irrespective of its precise age, this galaxy provides an apparently robust datapoint on the red envelope of galaxy evolution. The quality of the Keck spectrum of 53W091 has encouraged several authors to attempt a detailed age determination of its stellar population. The initial analysis by Dunlop et al. (1996) indicated an age in the range 3–4 Gyr (for solar metallicity), and this was supported by the more detailed investigation of Spinrad et al. (1997). Such an age is only consistent with its high redshift in certain cosmologies, requiring a low-density Universe ($\Omega_0 \sim 0.2$), or else an unacceptably low Hubble constant for critical density. Subsequently, Bruzual & Magris (1998) concluded in favour of a younger age based on the most recent models of Bruzual & Charlot, although detailed fitting with these models still indicates an age > 2.5 Gyr (Dunlop 1999). More recently Yi (1999) has concluded in favour of a minimum age of 2 Gyr. However, this age is derived from a model which has a metallicity of twice solar, and if solar metallicity is assumed the age rises to > 3 Gyr. In summary, detailed age dating currently indicates that between 2 and 3.5 Gyr have elapsed since the last major epoch of star formation in 53W091, but irrespective of its precise age, 53W091 appears to be the best available example of a passively evolving elliptical galaxy at $z \simeq 1.5$.

Given this background, it therefore came as a major surprise when unpublished polarimetric data was recently reported as indicating that 53W091 has a very high infrared polarization – of order 40 per cent (Chambers, private communication). This measurement suggested that very little of its observed infrared light was contributed by stars, a result completely at odds with the predicted infrared luminosity of the stellar population based on the above-mentioned analyses of the ultraviolet SED. A major objective of the observations presented here was therefore to attempt to confirm or refute this result.

2.2 MRC 0156–252

Eales & Rawlings (1996) have compared radio galaxies at redshifts $z \sim 1$ and $z > 2$, and find that those radio galaxies at $z > 2$ have brighter absolute V -band magnitudes. Such a result might be attributed either to strong evolution in the stellar population of radio galaxies, or to an increasing misclassification of quasars as radio galaxies at higher redshifts.

MRC 0156–252 has the brightest known absolute V -band magnitude for a radio galaxy at $z \sim 2$. The cause of its high luminosity is uncertain: it may be being viewed during an epoch of intense star formation, or it may be a quasar obscured by dust (Eales & Rawlings 1996). Broad $\text{H}\alpha$ lines suggest that some of its light is originating in an

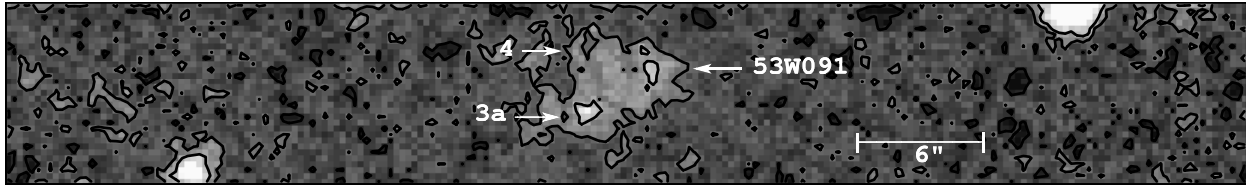


Figure 1. 53W091 - stacked *K*-band image of August 1997 and July 1997 data, total integration time 5 hours 56 minutes. [4 hours 4 minutes (August) plus 1 hour 52 minutes (July).] Overlaid with contours at 8%, 16% and 24% of the peak intensity present in the image. (North is at the top, East at the left.)

active nucleus. McCarthy et al. (1990) earlier classified it as a radio galaxy and suggested (McCarthy 1993), on the basis of its red spectral energy distribution, that it was a galaxy at an advanced stage of evolution. The radio flux is 131 ± 13 mJy at 4.85 GHz (Griffith et al. 1994) and 1.39 ± 0.05 Jy at 408 MHz (Large et al. 1981).

MRC 0156-252 appears unresolved in our *K*-band image (Figure 2), verifying the findings of McCarthy, Persson & West (1992), who did, however, find extended structure in their visible-band images. Our polarimetry allows us to investigate whether *K*-band light has been scattered into our line of sight.

2.3 3C 441

3C 441 appears in a rich field (Figure 3) with five neighbours; identification of the radio core as object *a* is based on the observations of Riley, Longair & Gunn (1980) and is apparently confirmed by the work of McCarthy (1988) and of Eisenhardt & Chokshi (1990). The object labelled *a* follows the notation of Lacy et al. (1998), who identify objects *c* and *d* to the north-west of object *a* – these are not shown in the restricted declination of Figure 3, though object *c* was clearly visible in the data taken by L&E. The star *B* is labelled as in Riley et al. (1980), and the remaining objects are labelled *E* thru *J*.

Fabry-Perot imaging by Neeser (1996) shows that none of the other objects in the field lie within a velocity range $(-1460, +1180)$ km s^{-1} of 3C 441 itself, but Neeser (1996) questions whether the identification of 3C 441 is correct – arguing that it may in fact be our object *F*.

The recent 8 GHz radio map of 3C 441 (Lacy et al. 1998) supports the traditional identification of the radio core with object *a*, and shows that the North-West jet is deflected to the south where it would otherwise have encompassed object *c*. It is known that 3C 441 has a broad-band optical polarization which is roughly perpendicular to its radio structure (Tadhunter et al. 1992).

3 INSTRUMENTATION AND REDUCTION PROCEDURE

Polarimetric observations were obtained using IRPOL2, installed at UKIRT (the United Kingdom Infrared Telescope, Hawaii) as described in L&E. We took data on the nights of 1997 August 18 and 19. IRPOL2 makes use of a Wollaston prism to split the light into parallel beams of orthogonal polarization. For our 1997 run (unlike that documented in L&E) we made use of the instrument's focal plane mask. We

created mosaics of each source by combining seven 60-s exposures at horizontal spacings of $9''$ and vertical spacings of $\pm 1''$. The total exposure time (summed over all four waveplate settings) is listed in Table 1.

Data reduction was performed using the standard UKIRT IRCAMDR software to flat field the images, and IRAF to align and combine the mosaics. The images were then averaged to form a single image for each waveplate, as this gives the best signal-to-noise in the final polarimetry (Leyshon 1998; Maronna et al. 1992; Clarke et al. 1983). The 3C 441 data was then combined, at each waveplate position, with our stacked 1995 images. Results are summarised in Table 2.

As is recommended for polarimetry, the normalised Stokes parameters q and u are tabulated; the reference axis for IRPOL2 is that $q > 0, u = 0$ corresponds to a polarization orientation of 83° E of N and that for $q = 0, u > 0$, the polarization orientation is 128° . The reference axis was verified by observing the standard star HD 215806 (Whittet et al. 1992).

In order to produce the pictures of the three sources presented here (Figures 1, 2 and 3) the upper and lower images from the final mosaics from all the waveplate positions were combined to form unpolarised images with the maximum depth; earlier data were also included, where available, as noted in the figure captions.

4 RESULTS AND DISCUSSION

4.1 The fraction of light arising in the nucleus

As discussed in L&E, the fraction Φ_K of the *K*-band observed light arising in the active nucleus is given by $\Phi_K = P_K / P_{Q,K}$, where P_K is the observed polarization and $P_{Q,K}$ is the undiluted polarization of the nuclear component scattered towards Earth. Models (Manzini & di Serego Alighieri 1996) suggest that the intrinsic polarization for realistic scattering by dust (at 90°) will be such that $1/P_{Q,K} = 2.5 \pm 0.5$, while electron scattering at any angle greater than 45° will give $1/P_{Q,W} = 2 \pm 1$. It follows that $\Phi_K \lesssim 3P_K$, so we can calculate a 1σ upper limit on the fraction of *K*-band light arising in the active nucleus as 3 times the 1σ upper limit $P + \sigma_P$ on the polarization. These values are also given in Table 2.

4.2 LBDS 53W091

The *K*-band image of 53W091 which results from stacking all of our data is shown in Figure 1. The companion object

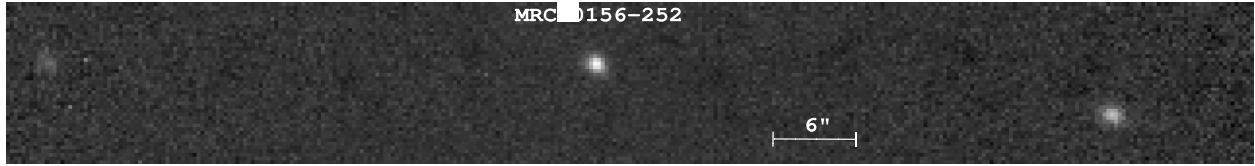


Figure 2. MRC 0156-252 - stacked *K*-band image of August 1997 data, total integration time 3 hours 44 minutes - including one cycle of observations which was not used for our subsequent polarimetry. (North is at the top, East at the left.)

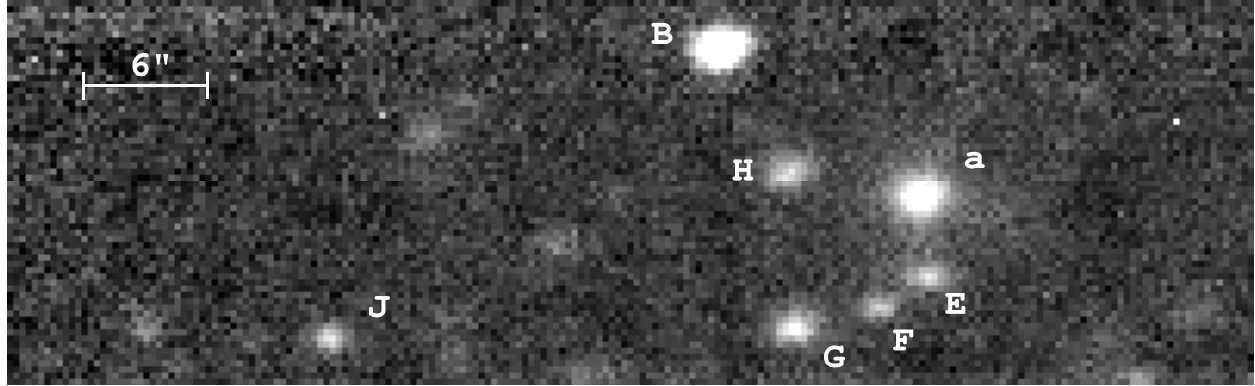


Figure 3. 3C 441 - stacked *K*-band image of August 1995 and August 1997 data, total integration time 4 hours 16 minutes. [1 hour 52 minutes (1997) plus 2 hours 24 minutes (1995).] (North is at the top, East at the left.) The objects are labelled as detailed in the text.

Table 3. B1950 co-ordinates of *K*-band sources in 53W091 field

Source	α	δ
53W091	17h 21m 17 ⁸ .898 \pm 0 ⁰ .057	+50° 08' 48 ^{''} .34 \pm 0 ⁰ .29
3a	17h 21m 18 ⁸ .156 \pm 0 ⁰ .029	+50° 08' 46 ^{''} .34 \pm 0 ⁰ .57

Key: α : B1950 Right Ascension; δ : B1950 Declination.

to the south-east of 53W091 appears to be at the same redshift, and is labelled '3a' in accordance with the labelling of Spinrad et al. (1997). The position of their third component is also marked (labelled '4'), although there is not a distinct source on our image.

Two stars on our image (the star on the top right of Figure 1 and a brighter one in the lower slot of the focal plane mask, not shown) were identified with stars whose B1950 co-ordinates were obtained from the *Digitized Sky Survey* (Lasker et al. 1990). Offsetting from these stars, the B1950 co-ordinates of the *K*-band sources were obtained and are given in Table 3.

Spinrad et al. (1997) discuss whether 3a and 53W091 together form a system displaying the alignment effect, given that the axis connecting the two objects is at a position angle of 126°, (comparable to the radio axis at 131°), and that the diagonal distance between 53W091 and 3a is 4'', comparable to radio-lobe separation in the 4.86 GHz map of Spinrad et al. (1997). However, the visible position of 53W091 (with which our infrared position measurement is consistent) is midway between the two radio lobes (and thus presumably coincides with the radio core), while the visible/infrared position of object 3a lies just outside the SE lobe. Thus, while an interaction between the (brighter) SE lobe and object 3a may be influencing the optical/radio appearance of the complex, 53W091 would appear to be the

host galaxy of the central radio source. Furthermore, the visible/ultraviolet spectra of both sources suggest they are dominated by old stars, implying that both objects are distinct galaxies, and that any aligned light associated directly or indirectly with the active nucleus of 53W091 makes at most a minor contribution to the visible and infrared morphology of the complex. [This interpretation is supported by recent WFPC2/NICMOS imaging of 53W091 (Dunlop 1999).]

Polarimetry was performed on both 53W091 and on Object 3a; results for both are given in Table 2. Since the objects were very faint and close together, the photometry aperture was not chosen according to the method in L&E, but was set to a radius of 4 pixels (1''.1). We also attempted to prune the frames with the greatest noise from our data and repeated the polarimetric analysis. Results for both the natural (\natural) and 'despiked' (\flat) data are given in Table 2.

There is a weak indication that Object 3a is polarised, with a 70 per cent chance of the polarisation being genuine. If there truly is polarisation at a level of 10-15 per cent, then 30-45 per cent of the light from object 3a could be scattered, and the source could consist entirely of scattered light within the error bars. (Dust scattering and non-perpendicular electron scattering will not result in total linear polarization of the scattered light.)

Is it possible that a beam from 53W091 is being scattered by a cloud at the position of 3a? The geometry suggests that this cannot be the case, since the polarization orientation is around 140°, which is nearly parallel to the line connecting 3a to 53W091. If 3a were a knot induced by a beam emerging from 53W091, a polarization orientation nearer 30° would have been expected.

The core of 53W091 itself provides no evidence for polarization, and it would be very difficult to reconcile our

Table 1. Redshifts, integration times and extinctions for our sample of radio galaxies.

Source	IAU form	z	λ_r (μm)	t_{int}	l	b	A_B	p_K
LBDS 53W091	1721+501	1.552	0.86	364	76.9	+34.5	0.08	0.06
MRC 0156–252	0156–252	2.016	0.73	196	208.6	-74.8	0.00	0.00
3C 441	2203+292	0.707	1.29	†112	84.9	-20.9	0.34	0.24

Key: z : redshift; λ_r (μm): rest-frame equivalent of observed-frame 2.2μm; t_{int} (min) : total integration time (min) summed over all waveplate settings (†: 3C 441 data was pooled with L&E's 144 minutes from August 1995 giving 256 minutes in total) ; l (°): Galactic longitude (NED); b (°): Galactic latitude (NED); A_B : Blue-band extinction (magnitudes), from NED, derived from Burstein & Heiles (1982); p_K : maximum interstellar contribution to K -band polarization (per cent).

Table 2. Observational results from polarimetry of 3 radio galaxies and neighbouring objects in the K -band.

Source	r''	$q(\sigma_q)$ (%)	$u(\sigma_u)$ (%)	$P \pm \sigma_P$ (%)	$2\sigma_{\text{UL}}$	Prob	θ (°)	σ_θ (°)	Φ_K (%)
LBDS 53W091 \natural	1.1	0.08 (16.6)	-7.5 (22.1)	$0.37 \pm {}^L 7.80$	30.8	10.8	38.3	±59.6	25
LBDS 53W091 \flat	1.1	0.64 (16.2)	-3.42 (18.4)	$0.17 {}^{L,U}$	21.5	2.02	43.3	±60.0	(65)
Object 3a \natural	1.1	-11.9 (18.7)	16.5 (18.4)	$16.0 \pm {}^L 13.9$	43.2	70.2	145.9	±23.7	89
Object 3a \flat	1.1	-4.5 (20.5)	20.5 (19.8)	$9.75 \pm {}^L 21.4$	45.5	67.1	134.2	±36.4	93
MRC 0156–252	2.3	-2.54 (7.02)	1.09 (7.36)	$0.14 \pm {}^L 4.28$	10.44	14.2	161.4	±59.4	13
MRC 0156–252	2.7	-0.53 (7.57)	-0.54 (8.33)	$0.04 {}^{L,U}$	4.19	0.89	60.1	±60.0	(13)
MRC 0156–252	3.4	0.43 (8.44)	0.81 (9.38)	$0.05 {}^{L,U}$	5.49	1.00	114.0	±60.0	(16)
3C 441 a	3.1	3.89 (5.07)	-0.70 (4.97)	$1.03 \pm {}^L 6.30$	10.02	45.7	77.9	±50.5	22
3C 441 B \ddagger	3.1	0.53 (4.66)	-1.74 (4.69)	$0.09 \pm {}^L 2.80$	6.90	14.0	46.5	±59.4	9
3C 441 c \ddagger	3.1	1.26 (12.04)	10.01 (11.42)	$3.53 \pm {}^L 15.61$	23.94	54.1	124.4	±45.1	57
3C 441 E	2.6	5.44 (12.28)	19.02 (12.94)	$17.65 {}^{+9.31}_{-8.08}$	36.24	90.5	120.0	±14.9	81
3C 441 F	2.0	5.85 (19.20)	16.41 (21.69)	$5.54 \pm {}^L 27.54$	43.25	48.4	118.2	±47.6	99
3C 441 G	2.6	-0.05 (12.74)	-5.90 (13.13)	$0.29 \pm {}^L 9.90$	20.52	18.3	37.7	±59.2	31
3C 441 H	2.3	-12.06 (14.02)	-8.85 (14.83)	$6.65 \pm {}^L 22.22$	32.63	66.5	11.1	±37.5	87
3C 441 S	2.3	0.37 (1.97)	-0.23 (1.96)	$0.02 {}^{L,U}$	2.27	4.7	66.9	±59.8	(7)

Key: Source: Source name and component (\natural : natural image; \flat : ‘despiked’ image; \ddagger : data is based on 1995 observations only; S is a bright star below 3C 441 accessible on the 1997 frames only); r : radius of photometry aperture (arcseconds); $q \pm \sigma_q$, $u \pm \sigma_u$: normalized Stokes Parameters (per cent) with respect to 83° E of N; $P \pm \sigma_P$: percentage polarization (debiased) with 1 σ error (L — the 1 σ lower limit for polarization is zero; L,U — the 1 σ ‘confidence interval’ is identically zero even though the best point estimate polarization is non-zero); $2\sigma_{\text{UL}}$: 2 σ upper limit (in per cent) for polarization in objects unlikely to be polarised; Prob: the probability that there is underlying polarization; $\theta \pm \sigma_\theta$: Electric vector orientation E of N (°); Φ_K : 1 σ upper limit (per cent) to fraction of light arising in the nucleus, or (2 σ) limit where the 1 σ limit is zero.

data with a polarization as high as the 40 per cent which Chambers (private communication) has suggested. We can only conclude that this previous measurement was in error, and/or was not based on sufficient integration time to properly constrain the polarization of this source. Our measured polarization orientation is 38°, nearly perpendicular to the radio axis and line to object 3a, but this is only marginally significant with errors of ±60° on our formal measure of the polarization angle.

4.3 MRC 0156-252

The criterion used by L&E to select the aperture for polarimetry did not yield a unique result for this object, so photometry is given in Table 2 for apertures of radius 8, 10 and 12 pixels. In all cases the best point estimate of the polarization is less than 0.15 per cent; and for the 10 and 12 pixel apertures, the formal 1 σ confidence interval indicates that the source is totally unpolarised. At most, if we assume that the polarization is due to the scatterering of light originally travelling perpendicular to our line of sight, 16 per

cent of its K -band light is due to this component, and might be assumed to be arising in an active nucleus.

The most recent radio maps of MRC 0156–252 (Carilli et al. 1997, 4710 MHz and 8210 MHz) do not display the marked head-tail asymmetry characteristic of beamed quasars. Nevertheless, it is possible that MRC 0156–252 is an obscured quasar (Eales & Rawlings 1996); if this is the case, we must be looking close to ‘straight down the jet’ with a shallower scattering angle for infrared light. If this were the case, our scattering assumptions would be invalid and hence our upper limit for Φ_K would be an underestimate.

4.4 3C 441

Our 1995 polarimetry (L&E) of 3C 441 was inconclusive, so we took advantage of this observing run to obtain further data. Given the uncertainty posited by Neeser (1996) over the identification of 3C 441, and the interest in object *c* of Lacy et al. (1998), we measured the polarization of all the objects on the field. The 1995 and 1997 images were stacked together to obtain polarization measurements of objects *a*

Table 4. Polarization in 3C 441 in two epochs

Epoch	p (%)	θ ($^{\circ}$)
August 1995	0.26 + 8	-5 ± 59
August 1997	19 ± 13	13 ± 19

Key: p : Debiased polarization; θ : polarization orientation.

(the putative core of 3C 441) and E thru H ; the 1995 data alone was used to obtain polarization data on B and c .

The only object with a strong indication (90 per cent chance genuine) of polarization is E . The orientation is 120° , which would be roughly parallel with the radio jet – but the position angle which E makes with the presumed core a is close to 0° , which means that a model of E scattering light from a is possible. It would not be necessary for light from a to be beamed into E ; if E subtends only a small solid angle of the light emitted by a , any light from a scattered by E would be quasi-unidirectional.

The availability of data from two epochs makes a crude test of temporal variability possible. The data are presented in Table 4, and it is clear that the measurements in the two epochs are consistent within the errors. Variation of polarization over a two year span can neither be proven nor disproven. If it is safe to pool the data from both epochs, the best estimate polarization, for the presumed radio galaxy at a , is 1 per cent at 78° ; but there is a 54 per cent chance that a is unpolarised with this result being merely an artefact of the noise. Even our result for E has a ten percent chance of being a noise-induced spurious result.

4.5 Polarized companions?

The presence of the 3C 441 case – i.e. where a companion object seems to be polarized in a manner consistent with the scattering of light emanating from the radio-loud object – may be significant in the wake of recent high-resolution imaging polarimetry of high redshift radio galaxies. Tran et al. (1998) used the Keck I to obtain extended imaging polarimetry of 3C 265, 3C 277.2 and 3C 324. In all three cases, the polarization maps displayed bipolar fans of polarization vectors centred on the nucleus, perpendicular to the optical structure and misaligned by tens of degrees with the radio axis. Earlier structural information on one radio galaxy was obtained by di Serego Alighieri, Cimatti & Fosbury (1993); their V -band polarimetry of the $z = 0.567$ object 1336+020 showed perpendicular polarization in a northern knot and in extended emission, higher than in the core.

Contour maps of the three Tran et al. (1998) sources are provided, at levels relative to the peak intensity of the central knot, and all three sources include companion objects. Little or no polarization is seen in the bright (~ 20 per cent of peak) companions of 3C 277.2 and 3C 324. But in 3C 265, a faint companion object also exhibits the polarization seen in the fan – the object is a knot less than 8 per cent of peak intensity and lies beyond the extension of the V -band optical structure, in the same direction but unconnected with the optical core in contours down to 2 per cent of peak. Such a faint polarized knot could readily be identified with light redirected by a cloud of scattering particles.

Assuming an $\Omega_0 = 1.0, \Lambda = 0$ cosmology with $H_0 = h_0 \text{ km s}^{-1} \text{ Mpc}^{-1}$, $h_0 = 100$, the knot in 3C 265 which lies about $9''$ from the core, is separated from the core by about $36h_0$ kpc. The extended structure of 1336 + 020 of about $3''$ corresponds to $12h_0$ kpc. In comparison the 53W091 to $3a$ separation and the distance between 3C 441 a and E both correspond to approximately $16h_0$ kpc. [Angular to linear scale conversion factors are taken from Peterson (1997, Fig. 9.3).] So the structure of these companion objects is of comparable scale to those in the literature.

It is possible, therefore, that companion E to 3C 441 is an illuminated object scattering light in the manner of the extended structure seen in 3C 265 and 1336 + 020. A determination of the redshift of object E would be required, however, to confirm that its presence in the field is not merely a line-of-sight effect. The parallel polarization of companion $3a$ to 53W091 cannot be explained in this way; but the measurement is too marginal to invite a search for parallel polarization mechanisms without more examples being found first.

5 CONCLUSIONS

Polarimetry of faint objects requires long integration times. The time available has permitted us to rule out the existence of very high polarizations in all the objects studied, at least for light emitted along the line of sight to Earth. It would obviously still be possible for light emitted in other directions from these objects to be polarised. ‘Polarization’ mentioned in the following conclusions should be understood in the restricted sense of light leaving the source in the direction of Earth. Under the Unified Model, radio galaxies (a class of AGN assumed to be oriented with their jets perpendicular to that line of sight) would be more likely to display polarization originating in scattering or synchrotron radiation in the light travelling Earthwards than in directions closer to the jet.

In the case of MRC 0156–252, which lies beyond a virtually dust-free part of our own Galaxy, we can be reasonably certain that this radio galaxy is not polarised, and the K -band light has not been scattered before reaching us. If some of the K -band light has originated in the active nucleus, its contribution should be smaller than at visible wavelengths (Manzini & di Serego Alighieri 1996); this being the case, subtraction of our image or a synthetic symmetrical galaxy could well reveal the structure of the active component at visible wavelengths, given the visible structure observed by McCarthy et al. (1992).

In LBDS 53W091, we can rule out the contribution of an active nucleus to providing more than ~ 25 per cent of the observed light. The majority of its K -band light, therefore, must be presumed to be due to its stellar population, and its $R - K$ colour remains consistent with an age in the range $2.5 - 3$ Gyr. The nature of its companion object $3a$, possibly polarised and of unclear physical relationship with 53W091, warrants further investigation.

In 3C 441, the polarization from object E may indicate that E is scattering light from a (whose identification as the central engine would thus be vindicated); the orientation of E ’s polarization would not be consistent with the source being located within E or F and emitting jets at

$\sim 145^\circ$. Therefore, we favour the traditional identification of the central engine with a .

The presence of companion objects perpendicularly polarized to the line of sight may be providing our first hints of a near infrared scattering medium concentrated in clouds in the vicinity of active nuclei. Further studies are required, however, to establish the nature of particular companions, and the presence of near infrared companions as a whole.

Acknowledgements

We thank Antonio Chrysostomou for help with the observations, and an anonymous referee for useful suggestions. The United Kingdom Infrared Telescope is operated by the Joint Astronomy Centre on behalf of the U.K. Particle Physics and Astronomy Research Council. We thank the Department of Physical Sciences, University of Hertfordshire for providing IRPOL2 for the UKIRT.

This research has made use of the NASA/IPAC extragalactic database (NED) which is operated by the Jet Propulsion Laboratory, CalTech, under contract with the National Aeronautics and Space Administration. Data reduction was performed with STARLINK and IRAF routines. We acknowledge the use of NASA's *SkyView* facility (<http://skyview.gsfc.nasa.gov>) located at NASA Goddard Space Flight Center. GL thanks PPARC for a research award.

REFERENCES

Bruzual G., Magris G., 1998, in: *The Hubble Deep Field*, STScI Symp., in press, astro-ph/9707154

Burstein D., Heiles C., 1982, AJ, 87, 1165

Carilli C. L., Röttgering H. J. A., van Ojik R., Miley G. K., van Breugel W. J. M., 1997, ApJS, 109, 1

Cimatti A., Dey A., van Breugel W. J. M., Antonucci R., Spinrad H., 1996, ApJ, 465, 145

Cimatti A., Dey A., van Breugel W. J. M., Hurt T., Antonucci R., 1997, ApJ, 476, 677

Cimatti A., di Serego Alighieri S., Vernet J., Cohen M., Fosbury R. A. E., 1998, ApJ, 499, L21

Clarke D., Stewart B. G., Schwarz H. E., Brooks A., 1983, A&A, 126, 260

Chambers K. C., Miley G. K., van Breugel W. J. M., 1987, Nat, 329, 604

Dey A., Cimatti A., van Breugel W. J. M., Antonucci R., Spinrad H., 1996, ApJ, 465, 157

di Serego Alighieri S., Fosbury R. A. E., Quinn P. J., Tadhunter C. N., 1989, Nat, 341, 307

di Serego Alighieri S., Cimatti A., Fosbury, R. A. E., 1993, ApJ, 404, 584

Dunlop J. S., 1999, in: *The Most Distant Radio Galaxies*, KNAW Colloquium Amsterdam, pp. 71-84, eds. Röttgering H. J. A., Best P., Lehnert M. D., Kluwer, astro-ph/9801114

Dunlop J. S., Peacock J. A., 1993, MNRAS, 263, 936

Dunlop J. S., Peacock J. A., Spinrad H., Dey A., Jimenez R., Stern D., Windhorst R., 1996, Nat, 381, 581

Eales S. A., Rawlings S., 1996, ApJ, 460, 68

Eales S. A., Rawlings S., Law-Green D., Cotter G., Lacy M., 1997, MNRAS, 291, 593

Eisenhardt P., Chokshi A., 1990, ApJ, 351, L9

Griffith M. R., Wright A. E., Burke B. F., Ekers R. D., 1994, ApJS, 90, 179

Jannuzzi B., Elston R., 1991, ApJ, 366, L69

Lacy M., Rawlings S., Blundell K. M., Ridgway S. K., 1998, MNRAS, 298, 966 astro-ph/9803017

Large M. I., Mills B. Y., Little A. G., Crawford D. F., Sutton J. M., 1981, MNRAS, 194, 693

Lasker B. M., Sturch C. R., McLean B. J., Russell J. L., Jenkner H., Shara M. M., 1990, AJ, 99, 2019

Leyshon G., 1998, Exp. Astron., 8, 153, astro-ph/9709164

Leyshon G., Eales S. A., 1998, MNRAS, 295, 10 (L&E), astro-ph/9708085

Maronita R., Feinstein C., Clocchiatti, A., 1992, A&A, 260, 525

Manzini A., di Serego Alighieri S., 1996, A&A, 311, 79

McCarthy P. J., 1988, PhD thesis, University of California at Berkeley

McCarthy P. J., 1993, ARAA, 31, 639

McCarthy P. J., van Breugel W. J. M., Spinrad H., Djorgovski S., 1987, ApJ, 321, L29

McCarthy P. J., Dickinson M., Filippenko A. V., Spinrad H., van Breugel W. J. M., 1988, ApJ, 328, L29

McCarthy P. J., Kapahi V. K., van Breugel W. J. M., Subrahmanyam C. R., 1990, AJ, 100, 1014

McCarthy P. J., Persson S. E., West S. C., 1992, ApJ, 386, 52

Neeser M. J., 1996, PhD thesis, Ruprecht-Karls-Universität, Heidelberg

Peterson B. M., 1997, *An Introduction to Active Galactic Nuclei*, Cambridge University Press

Rawlings S., Lacy, M., Sivia D. S., Eales S. A., 1995, MNRAS, 274, 428

Rigler M. A., Lilly S. J., Stockton A., Hammer F., LeFèvre O. N., 1992, ApJ, 385, 61

Riley J. M., Longair M. S., Gunn J. E., 1980, MNRAS 192, 233

Robson I., 1996, *Active Galactic Nuclei*, Wiley, Chichester

Spinrad H., Dey A., Stern D., Dunlop J., Peacock J., Jimenez R., Windhorst R., 1997, ApJ, 484, 581

Tadhunter C. N., Scarrott S. M., Draper P., Rolph, C., 1992, MNRAS, 256, 53P

Tran H. D., Cohen M. H., Ogle P. M., Goodrich R. W., di Serego Alighieri S., 1998, ApJ, 500, 660

Whittet D. C. B., Martin P. G., Hough J. H., Rouse M. F., Bailey J. A., Axon D. J., 1992, ApJ, 386, 562

Yi S., 1999, ApJ, submitted